Nano Energy 22 (2016) 499–506

Contents lists available at ScienceDirect

Nano Energy

journal homepage: www.elsevier.com/locate/nanoen

Facile fabrication of three-dimensional TiO_2 structures for highly efficient perovskite solar cells

Segeun Jang [a,b,1], Jungjin Yoon [a,b,1], Kyungyeon Ha [a,b], Min-cheol Kim [a,b], Dong Hoe Kim [d], Sang Moon Kim [a,b], Seong Min Kang [a,b], Sei Jin Park [a,b], Hyun Suk Jung [c,*], Mansoo Choi [a,b,**]

[a] Department of Mechanical and Aerospace Engineering, Seoul National University, Seoul 151-742, Republic of Korea
[b] Global Frontier Center for Multiscale Energy Systems, Seoul National University, Seoul 151-744, Republic of Korea
[c] School of Advanced Materials Science and Engineering, Sungkyunkwan University, Suwon 440-746, Republic of Korea
[d] Chemical and Materials Science Center, National Renewable Energy Laboratory, CO 80401, USA

ARTICLE INFO

Article history:
Received 22 December 2015
Received in revised form
25 February 2016
Accepted 26 February 2016
Available online 3 March 2016

Keywords:
Aerosol
3-D nanostructure
PDMS
Perovskite
Light scattering
Charge collection

ABSTRACT

The capability of fabricating three dimensional (3-D) nanostructures with desired morphology is a key to realizing effective light-harvesting strategy in optical applications. In this work, we report a novel 3-D nanopatterning technique that combines ion-assisted aerosol lithography (IAAL) and soft lithography that serves as a facile method to fabricate 3-D nanostructures. Aerosol nanoparticles can be assembled into desired 3-D nanostructures via ion-induced electrostatic focusing and antenna effects from charged nanoparticle structures. Replication of the structures with a polymeric mold allows high throughput fabrication of 3-D nanostructures with various liquid-soluble materials. 3-D flower-patterned polydimethylsiloxane (PDMS) stamp was prepared using the reported technique and utilized for fabricating 3-D nanopatterned mesoporous TiO_2 layer, which was employed as the electron transport layer in perovskite solar cells. By incorporating the 3-D nanostructures, absorbed photon-to-current efficiency of $>95\%$ at 650 nm wavelength and overall power conversion efficiency of 15.96% were achieved. The enhancement can be attributed to an increase in light harvesting efficiency in a broad wavelength range from 400 to 800 nm and more efficient charge collection from enlarged interfacial area between TiO_2 and perovskite layers. This hybrid nanopatterning technique has demonstrated to be an effective method to create textures that increase light harvesting and charge collection with 3-D nanostructures in solar cells.

1. Introduction

Soft lithography is a technique for fabricating or replicating micrometer to nanometer scale structures using elastomeric stamps. Among the materials used in soft lithography, polydimethylsiloxane (PDMS) stamps are highly flexible and can be easily used to replicate micro- and nanoscale textures with high fidelity at low cost and high-throughput in comparison to energy-intensive patterning techniques such as photolithography, electron-beam lithography, and nanoimprint lithography. Soft lithography has been widely utilized in various research fields such as epidermal electronics [1], wearable sensors and actuators [2], piezoelectric and triboelectric nanogenerators [3,4], solar cell and light-emitting diode (LED) architectures [5,6], and microfluidic devices [7]. In solar cell architectures, it has been used to create light-harvesting features such as nanopatterned anti-reflection(AR) coatings on the front surface of the substrates [8] and to fabricate periodic nanostructures on the back surface of the substrate in order to enhance scattering of the red light into the active layer [9].

Soft lithography techniques usually employ Si masters made by top–down etching, whose patterns have been photolithographically defined. For this reason, their features are limited to straight extrusions of two-dimensional (2-D) patterns, and fabrication of truly 3-D nanostructures with polymeric stamps with complex morphology remains a challenge. Therefore, most light-scattering structures created using soft lithography have been relatively simple-shaped 2-D structures such as line-patterned gratings [10,11], and nanopillar arrays [12,13]. However, to realize an effective light-scattering and charge collection, employing 3-D nanostructures with complex morphology and high specific surface area is needed [14,15].

Many approaches have been developed to fabricate 3-D nanostructures, such as multiphoton lithography [16], holographic

* Corresponding author.
** Corresponding author at: Department of Mechanical and Aerospace Engineering, Seoul National University, Seoul 151-742, Republic of Korea
E-mail addresses: hsjung1@skku.edu (H.S. Jung), mchoi@snu.ac.kr (M. Choi).
[1] S. Jang and J. Yoon contributed equally to this work.

http://dx.doi.org/10.1016/j.nanoen.2016.02.050
2211-2855/

lithography [17], layer-by-layer technique with alignment based on electron beam lithography [18], colloidal sedimentation [19], and transfer printing [20]. Our group has previously developed ion-assisted aerosol lithography (IAAL) for constructing 3-D nanostructures [21]. IAAL is based on ion-assisted nanoparticle focusing and antenna effects from charged nanoparticle structures, and is able to produce complex 3-D nanostructures such as flower-like structures comprising multiple 'petals' [22], vertically standing matchstick-like structures [23], asymmetric structures [23], pyramidal structures [24], and bud-shaped structures [24]. Additionally, it has advantages of sub-micrometer resolution, high reproducibility, and wafer-scale production at room temperature and atmospheric pressure [24–26]. However, IAAL has limitations in terms of material choice, as materials used in IAAL should be discharged in aerosol form (nanoparticles dispersed in gas-phase medium), and is a relatively time consuming procedure which takes a few hours to complete.

Here, we demonstrate a novel strategy to create 3-D nanostructures with polymeric stamps by combining the strengths of IAAL and soft lithography. IAAL, which utilizes multi-spark discharge generator and cross-patterned substrate, enables fabrication of multiscale well-ordered 3-D nanostructures in a large area. Replication of completed 3-D nanostructures with polymeric stamps via soft lithography allows rapid production of 3-D nanostructures using various materials that the mold can be filled with.

To demonstrate the usage of 3-D nanostructure engineering in effective light-harvesting and charge collection scheme, the 3-D flower-shaped nanostructures from hybrid lithography were incorporated in perovskite solar cells. The perovskite cells have a great potential of becoming the next generation renewable energy source because of their high power conversion efficiency and low cost solution-based production, and have shown remarkable progress in the last decade [27–30]. So far, most of the effort has focused on investigating charge-carrier behaviors in the device structures (e.g. planar and mesoscopic structures) [31,32] and optimizing the deposition processes [33–36]. However, in order to further increase the performance of these cells, novel approaches to improve the optical responses are needed [37–40]. To the best of the authors' knowledge, there have not been many studies pertaining to patterning of mp-TiO_2 layer in perovskite solar cells with well-defined complex periodic structures to improve light harvesting and charge collection. Based on the hybrid nanopatterning technique, we fabricated a 3-D flower-shaped mesoporous TiO_2 (mp-TiO_2) layer via solvent-assisted molding and incorporated it into perovskite solar cells to improve light harvesting and charge collection.

2. Experimental details

The fabrication process of 3-D flower-shaped PDMS stamp via hybrid nanopatterning technique is shown in Fig. 1a–d. The process consists of three main parts: (1) fabrication of 3-D nanostructures through IAAL, (2) reinforcing the structures with spin-on-glass (SOG) coating, and (3) replication of the structures via soft lithography.

2.1. Fabrication of 3-D flower-shaped nanostructures

A multi-pin spark discharge generator was utilized to obtain uniform 3-D nanostructures over a large area. Fig. 1a shows our experimental setup, which consists of a spark discharge chamber,

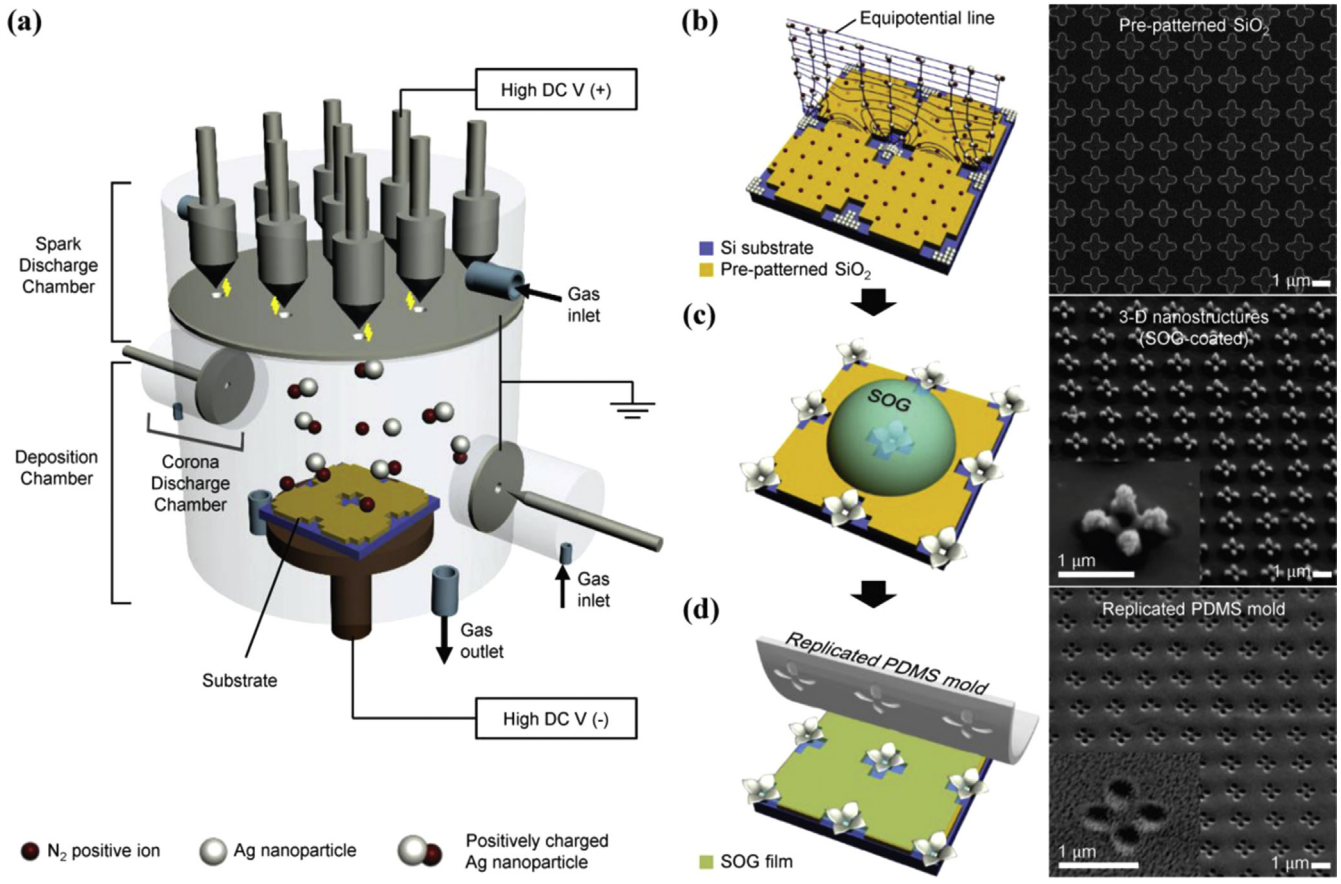

Fig. 1. Schematic illustration of (a) multi-pin spark discharge generator, and (b–d) preparation procedure of 3-D flower-patterned PDMS mold via hybrid lithography method and SEM images of the substrate in each step.

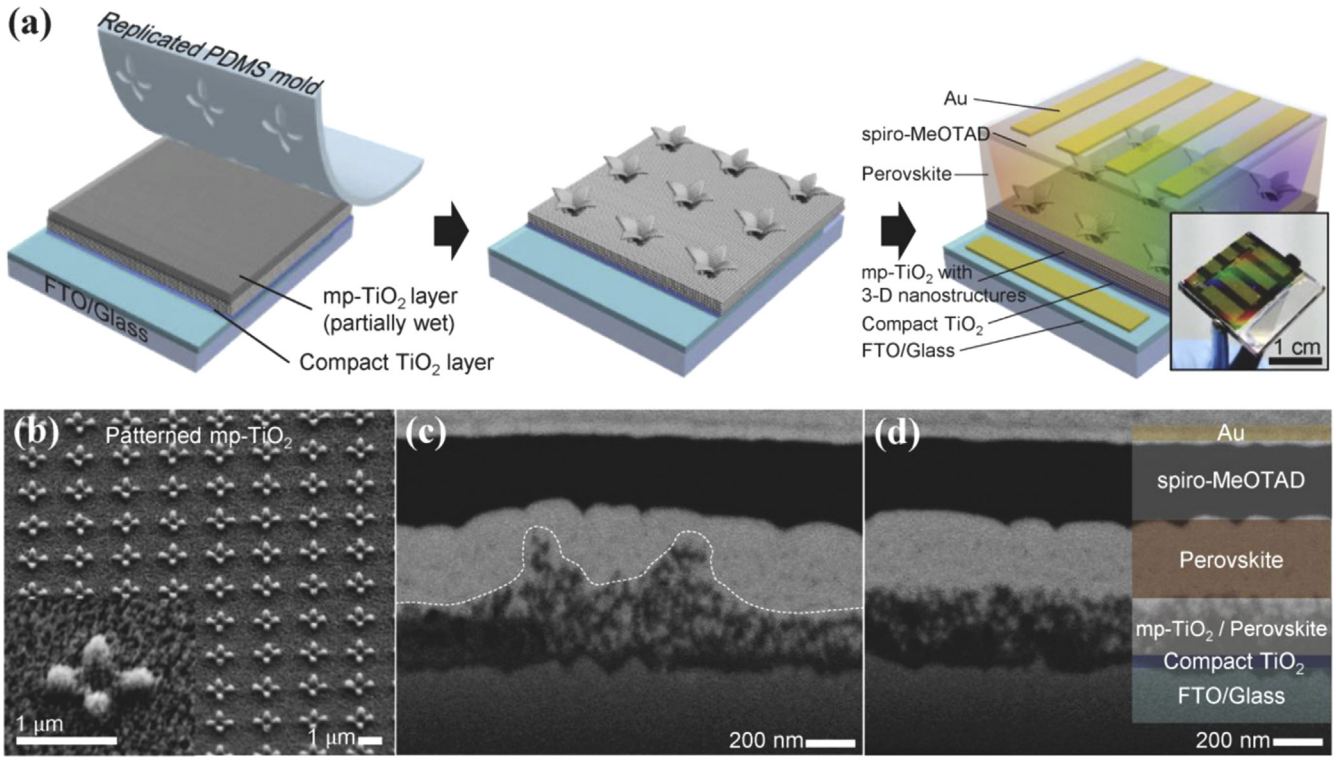

Fig. 2. (a) Schematic illustration of patterning of mp-TiO_2 using PDMS mold and perovskite solar cell with 3-D nanostructures (inset: photograph of completed device), (b) SEM image of 3-D nanopatterned mp-TiO_2, FIB-assisted cross-sectional SEM image for devices with (c) Patterned mp-TiO_2 and (d) Non-patterned mp-TiO_2.

a corona discharge chamber, and a deposition chamber. The spark discharge chamber is composed of tapered multi-pin Ag electrodes and a flat Ag plate with multi-hole. The gap between each pin and hole pair was set to 5 mm [24]. Applying a high DC voltage (~5 kV) to the multi-pin Ag electrode led to spark discharges between Ag pins and the grounded Ag plate, resulting in rapid evaporation of electrode material and generated positively charged Ag nanoparticles (NPs). These positively charged NPs were mixed with positive nitrogen ions, which were generated from the corona discharge chamber, and subsequently injected into the deposition chamber, where an electric field was formed between grounded inlets and sample substrate biased at −4 kV. As the electrical mobility of nitrogen ions is higher than that of positively charged Ag NPs, nitrogen ions accumulated on the patterned SiO_2 surface prior to the arrival of NPs. The nitrogen ions that have accumulated on the substrate induced a nanoscopic electrostatic lens effect [21]. Positively charged NPs were directed onto open Si surface following the deformed electric field streamlines and the accumulated NPs created additional attractive forces for subsequently arriving NPs via antenna effect. The combination of the forces caused the charged NPs to form 3-D flower-shaped nanostructures (Fig. 1b) [23]. As the morphology of pre-patterned SiO_2 surface determines the shape of the nanoscopic electrostatic lens and hence the final shape of the 3-D nanostructures, we carefully designed the SiO_2 pattern with cross-shaped openings that will result in flower-shaped structures that are 500 nm in width and length, 50 nm in height, in a square array with a 2 μm spacing (SEM image of Fig. 1b).

2.2. Fabrication of 3-D nanopatterned PDMS mold

Once the 3-D nanostructures were fabricated, they were replicated using PDMS mold. First, the nanostructures were reinforced with SOG to prevent structural damage during the replication process (Fig. 1c). Ag NPs making up the 3-D nanostructures are held together via weak van der Waal's force, hence the SOG-coating is needed to ensure the integrity of the structures during peel-off of the PDMS from the substrate. The substrate was spin-coated with SOG (Miraspin ED400A, APM Inc.) at 2000 rpm for 20 s and cured at 120 °C for 5 min and 250 °C for 30 min. Scanning electron microscopy (SEM) image of SOG-coated 3-D nanostructures is depicted in SEM image of Fig. 1c. Next, trichloro (1H,1H,2H,2H-perfluorooctyl) silane was evaporated onto the substrate to reduce the surface energy of SOG-coated 3-D nanostructures and allow easier detachment of the cured PDMS mold during the demolding process. Finally, PDMS (Sylgard 184, Dow Corning) was casted onto the substrate. The PDMS was mixed with a precursor to curing agent ratio of 10:1 and was detached from the substrate after being cured at 70 °C for 2 h (Fig. 1d). Also, SEM image shows the PDMS mold after peeling off from the substrate with 3-D nanostructures.

2.3. Fabrication of perovskite solar cells

Fluorine-doped Tin Oxide (TEC-8, Pilkington) substrate was cleaned with acetone, ethanol and deionized water in ultrasonic bath for 15 min, respectively. To deposit compact TiO_2 layer, the cleaned substrate was spin-coated with 0.15 M, 0.3 M of titanium diisopropoxide bis (acetylacetonate) (Sigma Aldrich) in 1-butanol (TCI) solution at 2000 rpm for 20 s and annealed at 500 °C for 30 min. Next, the 3-D nanopatterned mp-TiO_2 layer was fabricated by a molding process illustrated in Fig. 2a. A commercial TiO_2 paste (18NR-T, Dyesol) was diluted in anhydrous ethanol at a weight ratio of 5.5:1 and the solution was spin-coated on compact TiO_2 layer at 4000 rpm for 15 s. After spin-coating, the PDMS stamp was quickly placed on the surface of mp-TiO_2 layer so that the 3-D nanopatterned mp-TiO_2 can be formed by capillary action of the residual solvent in the spun layer. Then, the substrate was dried at 70 °C for 10 min to remove the residual solvent. The PDMS stamp was detached after drying and the substrate was annealed at

500 °C for 1 h. In the case of devices with unpatterned mp-TiO_2 layer, the molding process was not performed. The morphology of duplicated 3-D nanostructures on the mp-TiO_2 (Fig. 2b) showed high fidelity to the original 3-D nanostructures fabricated by IAAL (Fig. 1c). While not incorporated into the devices, other materials, both organic and inorganic, such as Ag nanoparticle ink (TEC-PR-020, Inktec) and PEDOT:PSS (Clevios PH1000, Heraeus) could also be patterned through same process (Fig. S1a and b). The perovskite layer was deposited by a solvent-engineering method reported by Jeon et al. [36]. A perovskite precursor solution was prepared by dissolving PbI_2 (Sigma Aldrich) and CH_3NH_3I which was synthesized according to the method by Stranks et al. [31] at a molar ratio of 1:1 in GBL (Sigma Aldrich) and DMSO (Sigma Aldrich) at a volume ratio of 7:3 and stirred at is 70 °C for 1 h. The prepared solution was spin-coated on mesoporous TiO_2 layer at 5000 rpm and toluene was drop-casted to obtain a uniform layer. Then the substrate was heated at 125 °C for 10 min. Subsequently, 25 μL of spiro-MeOTAD (Luminescence Technology) solution was spin-coated on perovskite layer at 4000 rpm for 30 s. The solution was prepared by dissolving 72 mg of spiro-MeOTAD in 1 mL chlorobenzene, 28.8 μL of 4-tert-butyl pyridine (Sigma Aldrich) and a solution of 720 mg of Li-TFSI in 1 mL acetonitrile (Sigma Aldrich). Finally, Au electrodes were deposited via thermal evaporation. Fig. 2c and d shows cross-sectional images of the complete device with and without 3-D nanostructures, respectively. Optical interference can be seen in the inset photograph of Fig. 2a showing the completed device, confirming the existence of the periodic 3-D nanostructures.

2.4. Morphological characterization

Surface images of 3-D nanopatterned substrate and cross-sectional images of perovskite solar cells were obtained using field-emission scanning electron microscope (AURIGA, Carl Zeiss) and each cross-sectional image was investigated with the aid of focused-ion-beam (FIB) system (AURIGA, Carl Zeiss) assisted with an energy selective backscattered detector to distinguish each layer which comprises the whole device more clearly.

2.5. Solar cell characterization

Current density–voltage (J–V) curves of the fabricated perovskite solar cells were measured using Keithley 237 under AM 1.5 G one-sun illumination provided by a solar simulator (Newport Oriel Sol 3A Class AAA, 64023A). Si-reference solar cell certified by NREL with KG-5 filter was used to calibrate the AM 1.5 G one-sun illumination condition. During the measurement, each device was covered by 2 mm × 5 mm rectangular metal aperture mask to set the active area to 0.10 cm^2. External quantum efficiency (EQE) curves were obtained using IQE-200 (Oriel) which combined a monochromatic light source and lock-in amplifier. Absorbance and reflectance spectra were recorded using Cary 5000 UV–visible spectrophotometer (Agilent technologies) in the wavelength range of 300–800 nm. Impedance spectroscopy was performed with electrochemical potentiostat CHI 600D (CH instruments).

3. Results and discussion

To investigate the optical enhancement provided by the 3-D flower-shaped nanostructures, the transmittance and reflectance spectra were measured (Fig. S2). Here the incident light was irradiated from the glass side and passed through FTO/compact TiO_2/mp-TiO_2 towards air. The reflectance of the substrate with patterned mp-TiO_2 layer was decreased by 10–15% over a broad wavelength range from 400 to 800 nm compared to that of the unpatterned substrate due to the presence of the 3-D nanostructures. The transmittance was increased by up to ~3.6% over the same visible wavelength range, corresponding to the trend shown by reflectance measurements. These results indicate that our structures create an anti-reflection (AR) effect that suppresses the Fresnel reflection (in other words, increase forward scattering) of incident light at the interface of mp-TiO_2/air, which means that their curved surfaces and complex morphology reduced the effect of the abrupt change of refractive index at the interface and can be utilized to enhance light harvesting in perovskite solar cells.

We fabricated and tested 29 perovskite solar cells incorporating the 3-D nanopatterned mp-TiO_2 layer to quantify the performance enhancement provided by the 3-D nanostructures. In Fig. 2a, a schematic illustration of the solar cell structure is shown. The photovoltaic characteristics of the fabricated devices are plotted in histograms shown in Fig. 3a. The average power conversion efficiency (PCE) of devices with 3-D nanostructures reached 13.59%, which is 10.30% higher than that of devices without the structures.

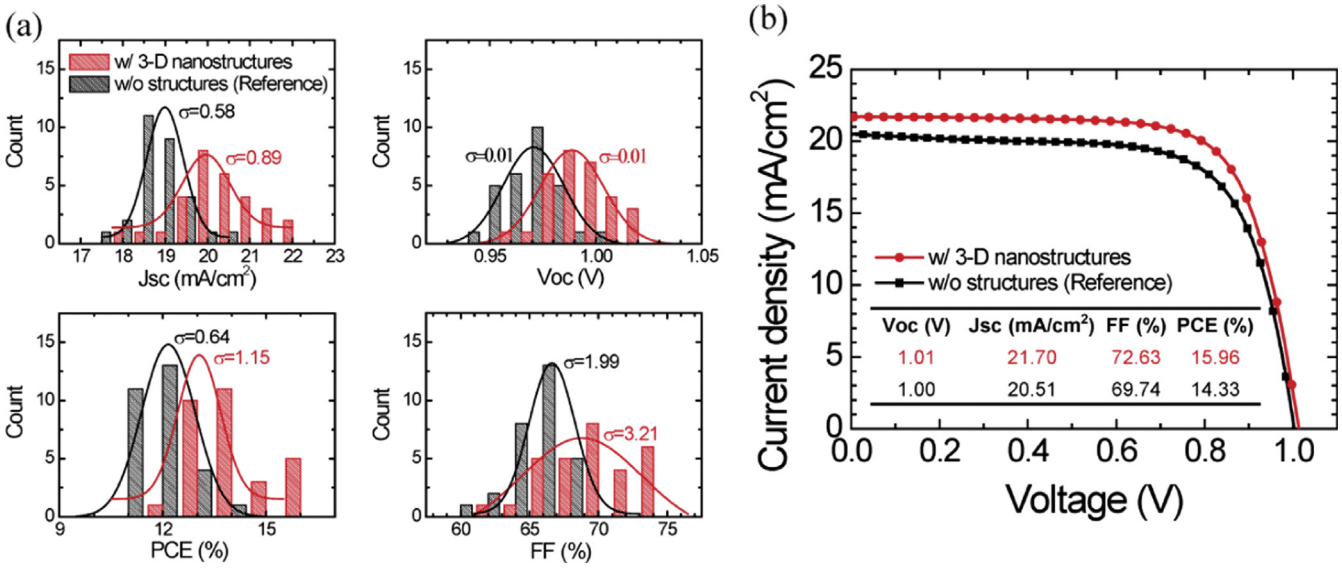

Fig. 3. (a) Histograms of device performance parameters (J_{SC}, V_{OC}, PCE, and FF) with standard deviation (σ) and (b) J–V curves of best performing perovskite solar cells with and without 3-D nanostructures.

Table 1
Summarized performance parameters of perovskite solar cells based on mp-TiO_2 structure. Average values were calculated from 29 devices with 3-D nanostructures and 29 devices without structures.

	J_{sc} (mA/cm^2)	V_{oc} (V)	FF (%)	PCE (%)	R_s (Ω)	R_{sh} (Ω)
w/nanopattern	20.06	0.99	68.35	13.59	61	33540.58
w/o nanopattern	19.09	0.97	66.42	12.32	64.63	14957.26

The average values of J_{SC}, open circuit voltage (V_{OC}), fill factor (FF), and PCE are summarized in Table 1. The best performing devices exhibited PCE of 15.96% with the nanostructures and 14.33% without the nanostructures, respectively, and their *J–V* curves are shown in Fig. 3b. By comparing the devices with and without the 3-D nanopatterned mp-TiO_2 layer, it can be seen that J_{SC}, V_{OC}, FF, and PCE were all increased by ~5%, ~2%, and ~3%, respectively. To elucidate the mechanism behind these improvements, further investigations of devices' optical and electrical properties were conducted.

The enhanced J_{sc} suggested improved light harvesting with nanostructured mp-TiO_2 layer, therefore the absorbance and reflectance spectra of glass/FTO/compact TiO_2/mp-TiO_2/perovskite substrates with and without 3-D nanostructures were measured (Fig. 4a). The reflectance decreased by 4–10% over almost the entire visible spectrum, signifying an increase of light absorption in perovskite layer over this range. To consider both changes in absorbance and reflectance simultaneously, light harvesting efficiency (LHE) was calculated by the following equation [41]:

$$\mathrm{LHE} = (1 - R)(1 - 10^{-A}) \quad (1)$$

where *R* is reflectance and *A* is absorbance. Fig. 4b shows LHE and LHE enhancement spectra of devices with and without 3-D nanostructures. The LHE increased by up to ~5.2% over the wavelength range of 400–800 nm with 3-D nanopatterned mp-TiO_2. A higher LHE value indicates that more incident photons reached the inside of the devices. The increase in LHE can be attributed to increased light harvesting due to extra scattering centers introduced by the flower-shaped morphology of the mp-TiO_2 layer [41], as well as the aforementioned AR effect provided by 3-D nanostructures. The AFM measurements show that the surface of 3-D nanopatterned mp-TiO_2 layer preserved the 3-D flower-shaped morphology (Fig. S3). In order to confirm current matching and enhanced light absorption, the external quantum efficiency (EQE) spectra (Fig. 4c) of the devices with and without the 3-D nanostructures were measured, showing enhanced EQE over the range of 400–800 nm which is consistent with the LHE enhancement. Integrated J_{SC} from these EQE spectra are calculated to be 19.18 mA cm^{-2} and 17.83 mA cm^{-2} for devices with and without 3-D nanostructures, respectively. Therefore, the EQE enhancement can be attributed to the AR effect and increased internal light scattering (light trapping) due to the enlarged interfacial area provided by 3-D nanostructures.

In addition, the presence of 3-D nanostructures in the mp-TiO_2 layer is expected to enhance charge transport. To quantify this effect, absorbed photon-to-electron conversion efficiency (APCE) was calculated from EQE and LHE using the following equation [41]:

$$\mathrm{APCE} = \mathrm{EQE}(\%)/\mathrm{LHE}(\%) \quad (2)$$

Fig. 5a shows the APCE spectra of the tested devices. APCE values of perovskite solar cells with the 3-D nanostructures were close to 100% at 650 nm, which was an increase of 10% compared to those of unpatterned device from 600 to 750 nm. This can be attributed to the enlarged interfacial area of mp-TiO_2/perovskite due to 3-D nanostructures playing a more effective role in extracting photogenerated electrons from the perovskite than a conventional flat mp-TiO_2 [42]. Also, the periodic protrusion of the 3D-nanostructures in the mp-TiO_2 layer would provide shorter electron pathways and consequently allow more electrons generated near the interface of perovskite/spiro-MeOTAD to reach mp-TiO_2 layer [14]. The protrusion morphology of our structures is confirmed by comparing the cross-sectional images of the devices of 3-D nanopatterned (Fig. 2c) and unpatterned (Fig. 2d) mp-TiO_2. It is noted that a thick mp-TiO_2 has a strong light absorption but low perovskite pore-filling and slow charge collection, while a thin mp-TiO_2 has better charge transport properties but relatively worse light harvesting and large hysteresis [36,43,44]. In this regard, mp-TiO_2 layer of proper thickness with protruded 3-D nanostructures can improve charge transport as well as light harvesting in mesostructured perovskite solar cells.

As demonstrated by the dark *J–V* curves in Fig. S4, perovskite solar cell with 3-D nanopatterned mp-TiO_2 showed a higher dark current onset as compared to conventional one. It indicates that 3-D TiO_2 structures effectively reduce the interface charge recombination [45,46]. Then, the effect of the 3-D nanopatterned mp-TiO_2 in perovskite solar cells with respect to its internal resistance was studied by obtaining the impedance spectra in frequency range 10 Hz to 1 MHz with 5 mV AC amplitude under AM 1.5 G one-sun illumination. Fig. 5b shows the Nyquist plots of the devices under three voltage conditions: 0 V, 0.8 V, and V_{OC}. The 3-D nanopatterned mp-TiO_2 based solar cells exhibited smaller radii of the semicircles across all voltage conditions, indicating that internal resistance of the device was reduced. Considering the resistance is inversely proportional to the area and the internal resistance is the sum of resistances of TiO_2/perovskite interface, TiO_2 itself, and FTO/TiO_2 interface, it is reasonable that enlarged interfacial area provided by 3D-nanostructures contributed to better contact and lower charge transport resistance at the interface of mp-TiO_2/perovskite [47,48]. The internal resistance of the devices can be represented by series resistance (R_s) and shunt resistance (R_{sh}) and these values are summarized in Table 1. The larger R_{sh} and smaller R_s of the devices with the 3-D nanostructures imply better charge transport, consistent with the

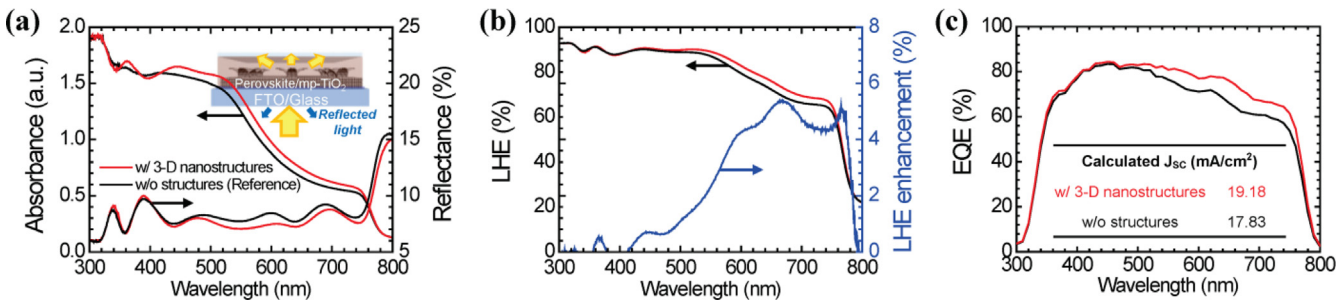

Fig. 4. (a) Absorbance and reflectance spectra, (b) LHE, and (c) EQE of perovskite solar cells with and without 3-D nanostructures. The enhancement of LHE corresponds to that of EQE, which accounts for increased J_{SC} by 3-D nanostructures.

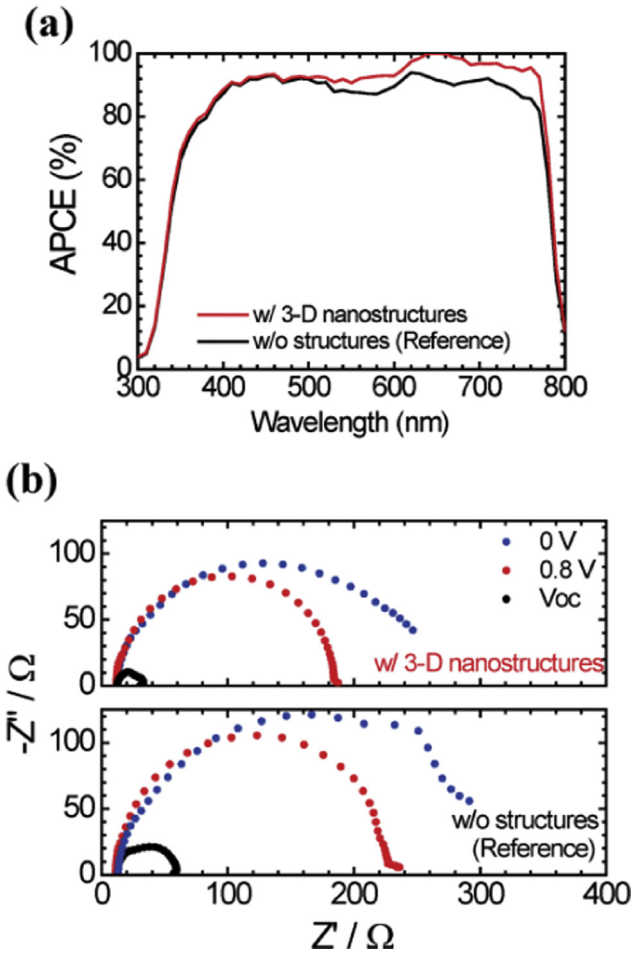

Fig. 5. (a) APCE and (b) Impedance spectra of devices with and without 3-D nanostructures measured under various voltage conditions. Increased APCE indicates that the internal charge collection was enhanced by the aid of 3-D nanostructures. Impedance measurements also show the decrease of internal resistance, which implies the enhanced charge transport ability.

previous observation. Therefore, by combining dark *J*–*V* test and impedance analysis, it is concluded that the 3-D nanopatterned mp-TiO_2 facilitates more effective charge transport compared to unpatterned mp-TiO_2 layer, yielding higher J_{SC}, FF, and V_{OC} [49,50].

Finally, the hysteresis of perovskite solar cells incorporating 3-D nanopatterned mp-TiO_2 was investigated (Fig. S5). *J*–*V* curves of forward and reverse scans lie almost perfectly on top of each other, indicating that the modified morphology of mp-TiO_2 layer in the perovskite solar cells does not cause significant hysteresis.

4. Conclusions

We have successfully developed a hybrid nanopatterning technique combining IAAL and soft lithography, and demonstrated its application in creating light harvesting and charge collecting structures in perovskite solar cells. The combination of the two different techniques allowed fabrication of well-ordered, 3-D flower-shaped nanostructures in a large area with high throughput using a variety of materials. Incorporation of 3-D nanostructures into mp-TiO_2 electron transporting layer led to perovskite solar cells with higher performance owing to increased J_{SC}, FF, and V_{OC}. J_{SC}, which affects PCE significantly, was increased due to more effective light harvesting provided by the periodic 3-D nanostructures. Furthermore, the enlarged interfacial area between TiO_2 and perovskite layers resulted in improved charge collection, leading to increases in J_{SC}, FF, and V_{OC}. As a result, about 10.3% improvement of average PCE was obtained on perovskite solar cells with 3-D TiO_2 nanostructures compared to those with flat TiO_2. Although the 3-D nanostructures produced by the developed nanopatterning technique were used for optimization of solar cells in this study, we believe that this technique will find further applications in optimization of various types of optoelectronic devices, such as photodetectors, light-emitting diodes, and solar water-splitting devices.

Acknowledgments

We thank Byeong Jo Kim for his insightful advice on the experimental methods. This work was supported by the Global Frontier R&D Program on Center for Multiscale Energy System funded by the National Research Foundation under the Ministry of Science, ICT & Future, Korea (Grants nos. 2011-0031561 and 2012M3A6A7054855).

Appendix A. Supplementary material

Supplementary data associated with this article can be found in the online version at http://dx.doi.org/doi:10.1016/j.nanoen.2016.02.050.

References

[1] D.-H. Kim, N. Lu, R. Ma, Y.-S. Kim, R.-H. Kim, S. Wang, J. Wu, S.M. Won, H. Tao, A. Islam, Science 333 (2011) 838–843.
[2] C. Pang, G.-Y. Lee, T.-I. Kim, S.M. Kim, H.N. Kim, S.-H. Ahn, K.-Y. Suh, Nat. Mater. 11 (2012) 795–801.
[3] K.-I. Park, S. Xu, Y. Liu, G.-T. Hwang, S.-J.L. Kang, Z.L. Wang, K.J. Lee, Nano Lett. 10 (2010) 4939–4943.
[4] F.-R. Fan, L. Lin, G. Zhu, W. Wu, R. Zhang, Z.L. Wang, Nano Lett. 12 (2012) 3109–3114.
[5] M.M. Tavakoli, K.-H. Tsui, S.-F. Leung, Q. Zhang, J. He, Y. Yao, D. Li, Z. Fan, ACS Nano (2015).
[6] L. Zhou, Q.-D. Ou, J.-D. Chen, S. Shen, J.-X. Tang, Y.-Q. Li, S.-T. Lee, Sci. Rep. 4 (2014).
[7] S.N. Bhatia, D.E. Ingber, Nat. Biotechnol. (2014).
[8] S.Y. Heo, J.K. Koh, G. Kang, S.H. Ahn, W.S. Chi, K. Kim, J.H. Kim, Adv. Energy Mater. 4 (2014).
[9] H.A. Atwater, A. Polman, Nat. Mater. 9 (2010) 205–213.
[10] J. Lee, M. Lee, Adv. Energy Mater. 4 (2014).
[11] S.-I. Na, S.-S. Kim, S.-S. Kwon, J. Jo, J. Kim, T. Lee, D.-Y. Kim, Appl. Phys. Lett. 91 (2007) 173509.
[12] S.I. Na, S.S. Kim, J. Jo, S.H. Oh, J. Kim, D.Y. Kim, Adv. Funct. Mater. 18 (2008) 3956–3963.
[13] V.E. Ferry, M.A. Verschuuren, H.B. Li, E. Verhagen, R.J. Walters, R.E. Schropp, H. A. Atwater, A. Polman, Opt. Express 18 (2010) A237–A245.
[14] J.H. Noh, H.S. Han, S. Lee, J.Y. Kim, K.S. Hong, G.S. Han, H. Shin, H.S. Jung, Adv. Energy Mater. 1 (2011) 829–835.
[15] S. Wooh, H. Yoon, J.H. Jung, Y.G. Lee, J.H. Koh, B. Lee, Y.S. Kang, K. Char, Adv. Mater. 25 (2013) 3111–3116.
[16] L.R. Meza, S. Das, J.R. Greer, Science 345 (2014) 1322–1326.
[17] M. Campbell, D. Sharp, M. Harrison, R. Denning, A. Turberfield, Nature 404 (2000) 53–56.
[18] M. Qi, E. Lidorikis, P.T. Rakich, S.G. Johnson, J. Joannopoulos, E.P. Ippen, H. I. Smith, Nature 429 (2004) 538–542.
[19] B. Hatton, L. Mishchenko, S. Davis, K.H. Sandhage, J. Aizenberg, Proc. Natl. Acad. Sci. 107 (2010) 10354–10359.
[20] J. Zaumseil, M.A. Meitl, J.W. Hsu, B.R. Acharya, K.W. Baldwin, Y.-L. Loo, J. A. Rogers, Nano Lett. 3 (2003) 1223–1227.
[21] H. Kim, J. Kim, H. Yang, J. Suh, T. Kim, B. Han, S. Kim, D.S. Kim, P.V. Pikhitsa, M. Choi, Nat. Nanotechnol. 1 (2006) 117–121.
[22] K. Jung, J. Hahn, S. In, Y. Bae, H. Lee, P.V. Pikhitsa, K. Ahn, K. Ha, J.K. Lee, N. Park, Adv. Mater. 26 (2014) 5924–5929.
[23] H. Lee, S. You, P.V. Pikhitsa, J. Kim, S. Kwon, C.G. Woo, M. Choi, Nano Lett. 11 (2010) 119–124.

[24] K. Ha, H. Choi, K. Jung, K. Han, J.-K. Lee, K. Ahn, M. Choi, Nanotechnology 25 (2014) 225302.
[25] S. You, K. Han, H. Kim, H. Lee, C.G. Woo, C. Jeong, W. Nam, M. Choi, Small 6 (2010) 2146–2152.
[26] C.G. Woo, H. Shin, C. Jeong, K. Jun, J. Lee, J.R. Lee, H. Lee, S. You, Y. Son, M. Choi, Small 7 (2011) 1790–1794.
[27] A. Kojima, K. Teshima, Y. Shirai, T. Miyasaka, J. Am. Chem. Soc. 131 (2009) 6050–6051.
[28] H.-S. Kim, C.-R. Lee, J.-H. Im, K.-B. Lee, T. Moehl, A. Marchioro, S.-J. Moon, R. Humphry-Baker, J.-H. Yum, J.E. Moser, Sci. Rep. 2 (2012).
[29] W.S. Yang, J.H. Noh, N.J. Jeon, Y.C. Kim, S. Ryu, J. Seo, S.I. Seok, Science (2015) aaa9272.
[30] N. Ahn, D.-Y. Son, I.-H. Jang, S.M. Kang, M. Choi, N.-G. Park, J. Am. Chem. Soc. 137 (2015) 8696–8699.
[31] S.D. Stranks, G.E. Eperon, G. Grancini, C. Menelaou, M.J. Alcocer, T. Leijtens, L. M. Herz, A. Petrozza, H.J. Snaith, Science 342 (2013) 341–344.
[32] M.M. Lee, J. Teuscher, T. Miyasaka, T.N. Murakami, H.J. Snaith, Science 338 (2012) 643–647.
[33] J. Burschka, N. Pellet, S.-J. Moon, R. Humphry-Baker, P. Gao, M.K. Nazeeruddin, M. Grätzel, Nature 499 (2013) 316–319.
[34] M. Liu, M.B. Johnston, H.J. Snaith, Nature 501 (2013) 395–398.
[35] J.-H. Im, I.-H. Jang, N. Pellet, M. Grätzel, N.-G. Park, Nat. Nanotechnol. 9 (2014) 927–932.
[36] N.J. Jeon, J.H. Noh, Y.C. Kim, W.S. Yang, S. Ryu, S.I. Seok, Nat. Mater. (2014).
[37] N. Marinova, W. Tress, R. Humphry-Baker, M.I. Dar, V. Bojinov, S. M. Zakeeruddin, M.K. Nazeeruddin, M. Grätzel, ACS Nano 9 (2015) 4200–4209.
[38] W. Zhang, M. Saliba, S.D. Stranks, Y. Sun, X. Shi, U. Wiesner, H.J. Snaith, Nano Lett. 13 (2013) 4505–4510.
[39] M. Long, Z. Chen, T. Zhang, Y. Xiao, X. Zeng, J. Chen, K. Yan, J. Xu, Nanoscale (2015).
[40] S. Carretero-Palacios, M. Calvo, H. Míguez, J. Phys. Chem. C 119 (2015) 18635–18640.
[41] J.-W. Lee, S.H. Lee, H.-S. Ko, J. Kwon, J.H. Park, S.M. Kang, N. Ahn, M. Choi, J.K. Kim, N.-G. Park, J. Mater. Chem. A 3 (2015) 9179–9186.
[42] A. Yella, L.-P. Heiniger, P. Gao, M.K. Nazeeruddin, M. Grätzel, Nano Lett. 14 (2014) 2591–2596.
[43] Y. Zhao, A.M. Nardes, K. Zhu, J. Phys. Chem. Lett. 5 (2014) 490–494.
[44] T. Leijtens, B. Lauber, G.E. Eperon, S.D. Stranks, H.J. Snaith, J. Phys. Chem. Lett. 5 (2014) 1096–1102.
[45] W. Ke, G. Fang, J. Wang, P. Qin, H. Tao, H. Lei, Q. Liu, X. Dai, X. Zhao, ACS Appl. Mater. Interfaces 6 (2014) 15959–15965.
[46] S. Do Sung, D.P. Ojha, J.S. You, J. Lee, J. Kim, W.I. Lee, Nanoscale 7 (2015) 8898–8906.
[47] B.J. Kim, D.H. Kim, Y.-Y. Lee, H.-W. Shin, G.S. Han, J.S. Hong, K. Mahmood, T.K. Ahn, Y.-C. Joo, K.S. Hong, Energy Environ. Sci. 8 (2015) 916–921.
[48] K. Mahmood, B.S. Swain, A. Amassian, Adv. Energy Mater. 5 (2015) 1500568.
[49] S.H. Ko, D. Lee, H.W. Kang, K.H. Nam, J.Y. Yeo, S.J. Hong, C.P. Grigoropoulos, H. J. Sung, Nano Lett. 11 (2011) 666–671.
[50] W.L. Hoffeditz, M.J. Katz, P. Deria, A.B. Martinson, M.J. Pellin, O.K. Farha, J. T. Hupp, ACS Appl. Mater. Interfaces 6 (2014) 8646–8650.

Segeun Jang received his B.S. degree in mechanical engineering at Yonsei University in 2013, and he is currently a Ph.D. candidate in the school of mechanical and aerospace engineering at Seoul National University under the supervision of Prof. Mansoo Choi. His research has been focused on a novel way to fabricate multiscale and multifunctional structures for energy devices, including dye sensitized solar cells, perovskite solar cells, and polymer electrolyte membrane fuel cells.

Jungjin Yoon received his B.S. degree in mechanical engineering in Kyung Hee University in 2012 and he is currently a Ph.D. student in school of mechanical and aerospace engineering in Seoul National University. He has been working on optimization and characterization of perovskite solar cells with functionalized nanomaterials under the co-supervision of Professor Hyun Suk Jung and Professor Mansoo Choi.

Kyungyeon Ha received the B.S. (2009) in Mechanical System Design Engineering from Hongik University and Ph.D. (2015) degree in Mechanical Engineering from Seoul National University. She currently works for Global Frontier center for Multiscale Energy Systems as a postdoctoral fellow. Her current interests are in multiscale multidimensional nanoparticle assembly and its application of nanodevices.

Min-cheol Kim received his B.S. degree in mechanical engineering in Seoul National University (SNU) in 2013 and he is currently a Ph.D. student in the same department in SNU. He has been working on fabrication and characterization of functionalized perovskite solar cells under the co-supervision of Professor Hyun Suk Jung and Professor Mansoo Choi.

Dong Hoe Kim received his B.S., and Ph.D. from Seoul National University in Materials Science and Engineering in 2008, and 2015, respectively. Since then, he is a Postdoc Researcher with Dr. Kai Zhu in National Renewable Energy Laboratory. His research interests are synthesis of organic–inorganic hybrid light harvesting materials, and design of advanced photoelectrode for highly efficient photovoltaic.

Sang Moon Kim received his B.S. degree from the school of mechanical and aerospace engineering at Seoul National University (SNU) in 2010 and obtained his Ph.D. degree from the same department at SNU in 2015. He currently works for Global Frontier center for Multiscale Energy Systems as a postdoctoral fellow. His research interest is focused on the directional physicochemical properties of anisotropic micro/nanostructures and stimuli-responsive polymeric patterns for energy conversion device and actuation system.

Seong Min Kang received his B.S. in mechanical and aerospace engineering and Ph.D. degree in same department from Seoul National University (SNU) in 2010 and 2015, respectively. He is currently a postdoctoral fellow in Global Frontier Center for Multiscale Energy Systems. His research has been focused on multiscale design and fabrication of bioinspired multifunctional structures for superomniphobic surfaces and solar cells applications.

Sei Jin Park is a research fellow at the Global Frontier Center for Multiscale Energy Systems in Seoul National University (SNU). He received his B.S., M.S. and Ph.D. in mechanical engineering from University of Michigan in 2008, 2011, and 2014 respectively. He was a postdoctoral associate at Massachusetts Institute of Technology before joining SNU in 2014. His current research focusses on creating novel material architectures for functional surfaces and energy devices.

Hyun Suk Jung is an associate professor in the School of Advanced Materials Science & Engineering at Sungkyunkwan University (SKKU). He received his B.S., M.S., and Ph.D. degrees in materials science and engineering from Seoul National University (SNU), in 1997, 1999, and 2004, respectively. He worked at Los Alamos National Laboratory (LANL) as a postdoctoral researcher in 2005. He had worked at Kookmin University (KMU) since 2006 and joined SKKU in 2011. His research presently focuses on perovskite solar cells and flexible solar cells.

Mansoo Choi is a professor of Department of Mechanical and Aerospace Engineering at Seoul National University in South Korea since 1991. He obtained his Ph.D. degree in 1987 from University of California, Berkeley. He is currently the president of International Aerosol Research Assembly (IARA), the editor-in-chief of Journal of Aerosol Science, and the director of the Global Frontier Center for Multiscale Energy Systems. His research centers on the fabrication of multiscale energy devices via ion-assisted aerosol lithography and aerosol-based synthesis of novel nanomaterials.